A Locally Adaptive Ensemble Approach for Data-Driven Prognostics of Heterogeneous Fleets

Sameer Al-Dahidi[1], Francesco Di Maio[1], Piero Baraldi[1*], Enrico Zio[1,2]

[1] Energy Department, Politecnico di Milano, Via La Masa 34, 20156 Milan, Italy
[2] Chair System Science and the Energy Challenge, Fondation Electricité de France (EDF), CentraleSupélec, Université Paris Saclay, Grande Voie des Vignes, 92290 Chatenay-Malabry, France

Abstract. In this work, we consider the problem of predicting the Remaining Useful Life (*RUL*) of a piece of equipment, based on data collected from an heterogeneous fleet working under different operating conditions. When the equipment experiences variable operating conditions, individual data-driven prognostics models are not able to accurately predict the *RUL* during the entire equipment life. The objective of the present work is to develop an ensemble approach of different prognostics models for aggregating their *RUL* predictions in an adaptive way, for good performance throughout the degradation progression. Two data-driven prognostics models are considered, an Homogeneous Discrete-Time Finite-State Semi-Markov Model (*HDTFSSMM*) and a Fuzzy Similarity-Based (*FSB*) model. The ensemble approach is based on a locally weighted strategy that aggregates the outcomes of the two prognostic models of the ensemble by assigning to each model a weight and a bias related to its local performance, i.e., the accuracy in predicting the *RUL* of patterns of a validation set similar to the one under study. The proposed approach is applied to a case study regarding an heterogeneous fleet of aluminum electrolytic capacitors used in electric vehicles powertrains. The results have shown that the proposed ensemble approach is able to provide more accurate *RUL* predictions throughout the entire life of the equipment compared to an alternative ensemble approach, and to each individual *HDTFSSMM* and *FSB* models.

***Keywords*:** Fault Prognostics, Remaining Useful Life (*RUL*), Locally Adaptive Ensemble, Heterogeneous Fleet, Homogeneous Discrete-Time Finite-State Semi-Markov Model (*HDTFSSMM*), Fuzzy Similarity-Based (*FSB*) Model, Aluminum Electrolytic Capacitors.

Notation and list of acronyms

RUL	Remaining Useful Life	G_{final}	Number of degradation states including the failure state of equipment
$HDTFSSMM$	Homogeneous Discrete-Time Finite-State Semi-Markov Model	$\widehat{RUL}_j(HDTFSSMM)$	*RUL* prediction provided by the *HDTFSSMM* model for a test equipment at time t_j
FSB	Fuzzy Similarity-Based	g	Index of degradation state, $g = 1, \dots, G_{final}$
KNN	*K*-Nearest Neighbors	N_{max}	Number of *MC* simulation trials
MLE	Maximum Likelihood Estimation	$\bar{r}_{l-M+1:l}^{p_{train}}$	The l-th segment of length M of p_{train} reference trajectory, $l = 1, \dots, I_{p_{train}}, p_{train} = 1, \dots, P_{train}$
FIM	Fisher Information Matrix	$\bar{r}_{j-M+1:j}$	The j-th segment of length M of a test trajectory
MC	Monte Carlo simulation	$\delta_l^{p_{train}}$	Pointwise difference between $\bar{r}_{l-M+1:l}^{p_{train}}$ and $\bar{r}_{j-M+1:j}$
P	Number of pieces of equipment in the fleet	$S_l^{p_{train}}$	Measure of similarity between $\bar{r}_{l-M+1:l}^{p_{train}}$ and $\bar{r}_{j-M+1:j}$
p	Index of equipment in the fleet, $p = 1, \dots, P$	$S_{l^*}^{p_{train}}$	Largest similarity between the p_{train} trajectory and the j-th segment of a test trajectory at time t_{l^*}
I_p	Number of measurements of *p*-th equipment	$rul_{l^*}^{p_{train}}$	True *RUL* of the p_{train} trajectory at time t_{l^*}
l	Index of the measurement time, $l = 1, \dots, I_p$	t_F	Failure time of the p_{train} trajectory, $p_{train} = 1, \dots, P_{train}$
t_l	The l -th measurement time of an equipment	t_{l^*}	Last time instant of the segment $\bar{r}_{l^*-M+1:l^*}^{p_{train}}$ which has the maximum similarity with the test trajectory
M	Number of discrete time steps between two successive measurements, $t_l - t_{l-1}$	$v^{p_{train}}$	The weight assigned to the p_{train} reference trajectory in the *FSB* model, $p_{train} = 1, \dots, P_{train}$
P_{train}	Number of pieces of equipment in the fleet used for training	α, β	Parameters of the bell-shaped similarity function of the *FSB* model
p_{train}	Index of equipment used for training, $p_{train} = 1, \dots, P_{train}$	$\widehat{RUL}_j(FSB)$	*RUL* prediction provided by the *FSB* model for a test trajectory at time t_j
$I_{p_{train}}$	Number of measurements of p_{train} equipment	H	Number of individual prognostic models
P_{train}^c	Number of complete-run-to-failure equipment used for training	h	Index of the prognostic model, $h = 1, \dots, H$
P_{train}^{ic}	Number of incomplete-run-to-failure equipment used for training	w_j^h	Weight associated to the h-th prognostic model at time t_j
P_{valid}	Number of pieces of equipment in the fleet used for validation	b_j^h	Bias associated to the h-th prognostic model at time t_j
p_{valid}	Index of equipment used for validation, $p_{valid} = 1, \dots, P_{valid}$	$\widehat{rul}_{l^*}^{p_{valid}}(h)$	*RUL* prediction provided by the h-th prognostic model for a p_{valid} trajectory at time t_{l^*}
$I_{p_{valid}}$	Number of measurements of p_{valid} equipment	$rul_{l^*}^{p_{valid}}$	True *RUL* of the p_{valid} trajectory at time t_{l^*}
P_{test}	Number of pieces of equipment in the fleet used for testing	$\bar{r}_{l-M+1:l}^{p_{valid}}$	The l-th segment of length M of p_{valid} trajectory, $l = 1, \dots, I_{p_{valid}}, p_{valid} = 1, \dots, P_{valid}$
p_{test}	Index of equipment used for testing, $p_{test} = 1, \dots, P_{test}$	$d_l^{p_{valid}}$	Pointwise difference between $\bar{r}_{j-M+i}$ and $\bar{r}_{l-M+i}^{p_{valid}}$
$I_{p_{test}}$	Number of measurements of p_{test} equipment	$d_{l^*}^{p_{valid}}$	Minimum distance $d_l^{p_{valid}}$ of p_{valid} trajectory at time t_{l^*}
t_j	The j-th test time of a test equipment	$mae_{j,P_{valid}}^h$	Local mean absolute error obtained by the h-th prognostic model at time t_j of the P_{valid} trajectories
Z	Number of signals of each degradation trajectory	$me_{j,P_{valid}}^h$	Local mean error obtained by the h-th prognostic model at time t_j of the P_{valid} trajectories
z	Index of signal	Q_j^h	Score provided to the h-th prognostic model in the borda-count method at time t_j
$\bar{\bar{X}}$	Dataset matrix of the collected measurements	$\widehat{RUL}_j(ensemble)$	Ensemble *RUL* prediction of the *H* prognostic models at time t_j of a test trajectory
G	Number of degradation states (final consensus clusters) of equipment	ESR^{norm}	Capacitor degradation indicator
T_t^{ESR}	Capacitor temperature at which the *ESR* measurement has been performed at time t	$\widehat{rul}_j^{p_{test}}$	*RUL* prediction of the p_{test} capacitor at time t_j
T_t	Aging temperature experienced by the capacitor at time t	$rul_j^{p_{test}}$	True *RUL* of the p_{test} capacitor at time t_j
ω_t	Process noise representing the degradation process stochasticity at time t	$AI^{p_{test}}$	Average accuracy index of the p_{test} equipment

η_t	Random noise representing the measurement error at time t	AI	Average accuracy index of the P_{test} pieces of equipment
F	Coefficient which defines the degradation rate of the capacitor	t_{sw}	Possible switching time of the adaptive switching ensemble approach, $t_{sw} = [t_{sw}^{min}, t_{sw}^{max}]$
a, b, c	Parameters characteristics of the capacitor	t_{opt}	Optimum switching time of the adaptive switching ensemble approach

1. Introduction

In industries such as nuclear, oil and gas, chemical and transportation, unforeseen equipment failures are extremely costly in terms of repair costs, lost revenues, environmental hazards and human fatalities [1]. To anticipate failures and mitigate their consequences, predictive maintenance approaches are being developed, based on the assessment of the actual equipment degradation condition and on the prediction of its evolution for setting the optimal time for maintenance [1]–[4]. The underlying concept is that of failure prognostics, i.e., predicting the Remaining Useful Life (*RUL*) of the equipment undergoing degradation [5]–[8] (the amount of time the equipment can continue performing its functions under the operational and working conditions it will experience).

In practice, efficient failure prognostics avoids system failures and unscheduled shutdowns, helps performing efficient maintenance strategies and allows full exploitation of the equipment useful life. Hence, failure prognostics increases the system availability and safety, while reduces maintenance costs [5], [6], [8]–[10].

Approaches for *RUL* estimation can be generally categorized into model-based and data-driven [5], [6], [11]–[18]. Model-based approaches use physics-based models to describe the degradation behaviour of the equipment [8], [12], [19], [20]. For example, Gebraeel et al. [21] presented a degradation modeling framework for *RUL* prediction of rolling bearings under time-varying operational conditions; Li et al. [22], [23], proposed two prediction models of defect propagation in bearings; Luo et al. [17] developed a model-based prognostic technique that relies on an accurate simulation model for system degradation prediction and applied the developed technique to a vehicle suspension system. Despite the fact that these approaches have been shown capable of providing accurate prognostic results, the assumptions and simplifications on which they are based may pose limitations on their practical deployment [7], [12], [24]–[26]. On the other side, data-driven prognostic approaches do not use any explicit physics-based model, but rely exclusively on the availability of process data related to equipment health to build (black-box) models that capture the degradation and failure modes of the equipment [5], [8], [20], [25], [27]–[30].

In this work, the availability of condition monitoring data from similar pieces of equipment, forming what in the industrial context is called a fleet [31], [32], motivates the development of data-driven

prognostic approaches that capitalize on the information contained in such data to estimate the equipment *RUL*. In practice, heterogeneous fleets of *P* pieces of equipment, which have different and/or similar technical features, typically undergo different usages under different operating conditions. Thus, even if the fleet data can provide wider knowledge concerning the equipment behaviour and, thus, can, in principle, improve the efficiency of the fault prognostics task [31]–[33], they are difficult to be treated within traditional data-driven prognostics schemes.

The main difficulty in prognostics tasks using fleet data is that the equipment typically experiences different operating conditions, which influence both the condition monitoring data and the degradation processes [34]. Therefore, individual data-driven prognostic models might not provide satisfactory *RUL* predictions in terms of accuracy: each model can provide accurate *RUL* predictions under some operating conditions but less accurate in others [35]. To overcome this, ensemble approaches, based on the aggregation of multiple model outcomes, have been introduced, with superior robustness and accuracy than the individual models [36], [37] and the possibility of estimating the uncertainty of the predictions [38].

The present work proposes an ensemble formed by different data-driven prognostics models, capable of aggregating the *RUL* predictions in an adaptive way, for good performance throughout the entire degradation trajectory of an equipment.

Two data-driven prognostics base models are considered: 1) an Homogeneous Discrete-Time Finite-State Semi-Markov Model (*HDTFSSMM*) [10], [34] and 2) a Fuzzy Similarity-Based (*FSB*) model [24]. The former approach entails building a statistical model of degradation, estimating its parameters and using the model within a direct Monte Carlo (*MC*) simulation scheme [39] to estimate the equipment *RUL*, whereas the latter model evaluates the similarity between the test degradation trajectory and the available fleet run-to-failure training trajectories, and uses the *RULs* of these latter to estimate the *RUL* of the former, considering how similar they are [24], [40]–[42].

The ensemble approach developed tailors the local fusion method developed in [43] to the scope of *RUL* aggregation. It is based on the following main four steps:

1) retrieve patterns from the validation set similar to the test pattern under analysis for the prediction. The retrieved validation patterns will be used for optimizing the values of the local fusion method, i.e., the weights in Step 2) and the biases in Step 3));
2) assign a weight to each individual model of the ensemble; the weight is proportional to the model prediction accuracy estimated on the retrieved patterns;

3) quantify the bias of each individual model of the ensemble; the bias is proportional to the model average *RUL* prediction error estimated on the retrieved patterns;
4) aggregate the outputs, accounting for the models weights and biases.

With respect to Step 1), a novel strategy is proposed for the identification of the patterns of the validation set similar to the test pattern. In [43], the similar patterns are those with the smallest distance from the test pattern under analysis, regardless of the degradation trajectory they belong to. This might cause identifying all the similar patterns in the same degradation trajectory and, thus, the ensemble approach might provide less accurate *RUL* predictions. This can be justified by the fact that the prediction accuracy of each individual model of the ensemble depends on the diversity and representativeness of the identified patterns that influences the weights assigned to the models. In other words, all degradation trajectories of the validation set can, in principle, bring useful information for determining the *RUL* of the test trajectory currently developing. Therefore, the proposed strategy considers at most only one similar pattern from each validation trajectory.

With respect to Step 2), three weighting strategies have been considered:

a) weight proportional to the inverse of the mean absolute error (*mae*) made by the model on the identified patterns of the validation set similar to the test pattern [43];

b) weight proportional to the logarithm of the inverse of the *mae* [43];

c) the borda-count method [36].

The quantification of the bias of each model in Step 3) consists in calculating the local mean error made by the model on the identified patterns of the validation set similar to the test pattern [43].

With respect to Step 4), the output aggregation is performed by a weighted average of the individual model *RUL* prediction to which the model local bias (Step 3) is subtracted, with the weights computed in Step 2).

Thus, the original contributions in this work are twofold:

1) the application of the local fusion method [43] for fault prognostics task;
2) the proposal of a new method for selecting patterns of the validation set most similar to the test pattern.

The proposed approach is applied to a case study regarding an heterogeneous fleet of aluminum electrolytic capacitors used in electric vehicles powertrains. The performance of the proposed approach is verified with respect to the Accuracy Index (*AI*) [44] and is compared with the performance of each individual model. For further comparison, an alternative ensemble approach is

applied to the case study and its results are compared to those obtained by the individual models and the proposed ensemble approach. The alternative approach is an adaptive switching ensemble approach for data-driven prognostics that selects the *HDTFSSMM* at early stages of life and the *FSB* model at the last stages of life [34], [45].

The remaining of this paper is organized as follows. In Section 2, the two prognostic models are briefly recalled. In Section 3, the proposed ensemble approach for the accurate estimation of the *RUL* of equipment belonging to an heterogeneous fleet working under variable operating conditions is illustrated. In Section 4, a case study regarding an heterogeneous fleet of aluminum electrolytic capacitors used in electric vehicles powertrains is described, and the results obtained with the proposed ensemble approach are discussed and compared with each individual model and an alternative adaptive switching ensemble approach. Finally, some conclusions are drawn in Section 5.

2. The Data-Driven Prognostics Models

This Section briefly illustrates the two data-driven prognostics models considered: the Homogeneous Discrete-Time Finite-State Semi-Markov Model (*HDTFSSMM*) (Subsection 2.1) proposed by some of the authors in [10], [34] and the Fuzzy Similarity-Based (*FSB*) model (Subsection 2.2) [24], respectively.

Let us assume that we have available I_p measurements for each one of the $p = 1, \dots, P$ pieces of equipment of an heterogeneous fleet monitored at predefined times $t_1, t_2, \dots, t_l, t_{I_p}$, $l = 1, \dots, I_p$. The time interval $t_l - t_{l-1}$ between two measurements is assumed to be formed by M discrete time steps. The P pieces of equipment are divided into P_{train} training, P_{valid} validation and P_{test} test sets for the purpose of building the individual models, developing the proposed ensemble approach and verifying its performance, respectively. Each p-th trajectory is a Z-dimensional trajectory, where Z is the number of signals representative of the equipment behaviour and of the operating conditions that the equipment is subjected to. Among the training trajectories, P_{train}^{c} are complete run-to-failure trajectories (i.e., trajectories that last all the way to the instance when the degradation state reaches the threshold value beyond which the equipment loses its functionality) and $P_{train}^{ic} = P_{train} - P_{train}^{c}$ are incomplete run-to-failure trajectories (i.e., trajectories that do not reach the failure threshold).

2.1. The Homogeneous Discrete-Time Finite-State Semi-Markov Model (*HDTFSSMM*)

The degradation process is assumed to follow an Homogenous (i.e., memoryless), Discrete-Time (i.e., transitions among states occur at discrete time instants), Finite-State (i.e., a finite set of degradation states) and Semi-Markov (i.e., transition rates depend on the current state sojourn time with any arbitrary distribution) model [46]–[49]. The transition rates are taken as discrete Weibull distributions, as these are the probability distributions most commonly used to describe degradation processes of industrial equipment [10], [48], [50].

The flowchart for the method is sketched in Figure 1. The method goes along the following two phases: a training phase for building the degradation model and estimating its parameters and a test phase for using the model within a direct Monte Carlo (*MC*) simulation scheme to estimate the *RUL* of an equipment. Overall, it entails three main steps [10], [34]:

Step 1: *Setting up the number of states of the HDTFSSMM*. The multidimensional segments of measurements taken from the P_{train} degradation trajectories are appended in the matrix $\bar{\bar{X}}$. The objective is to partition the collected data in $\bar{\bar{X}}$ into G dissimilar groups (whose number is "a priori" unknown), such that data belonging to the same group characterize the degradation states of the *HDTFSSMM* that has to be built.

To this aim, an unsupervised ensemble clustering approach is adopted (refer to [51]–[53] for more details): two base clusterings are first performed on two groups of signals (the first populated by signals representative of the equipment behaviour and the second representative of the operating conditions) and, then, ensembled to get the final consensus clusters G that can be seen as the states representative of the different degradation levels of the equipment, that are influenced and explained by different operating conditions [51]. The failure state (i.e., an absorbing state) at which the degradation level reaches the failure threshold value is added to those states to build the transition diagram of the equipment operation with G_{final} states (i.e., $G_{final} = G + 1$ states).

Phase 2: *States transition parameters estimation and their uncertainty quantification*. Once the topology of the model is fully defined, the parameters governing the transitions among the degradation states and their uncertainty are to be estimated by resorting to the Maximum Likelihood Estimation (*MLE*) technique and the Fisher Information Matrix (*FIM*), respectively (refer to [54] for more details).

Phase 3: *Direct Monte Carlo (MC) simulation of the degradation progression for the online estimation of the RUL*. At the current time t_j, the *RUL* provided by the *HDTFSSMM* model

$\widehat{RUL}_j(HDTFSSMM)$ of a test equipment is estimated using the M latest measurements of the Z-dimensional signals and by resorting to the direct *MC* simulation with N_{max} trials [55].

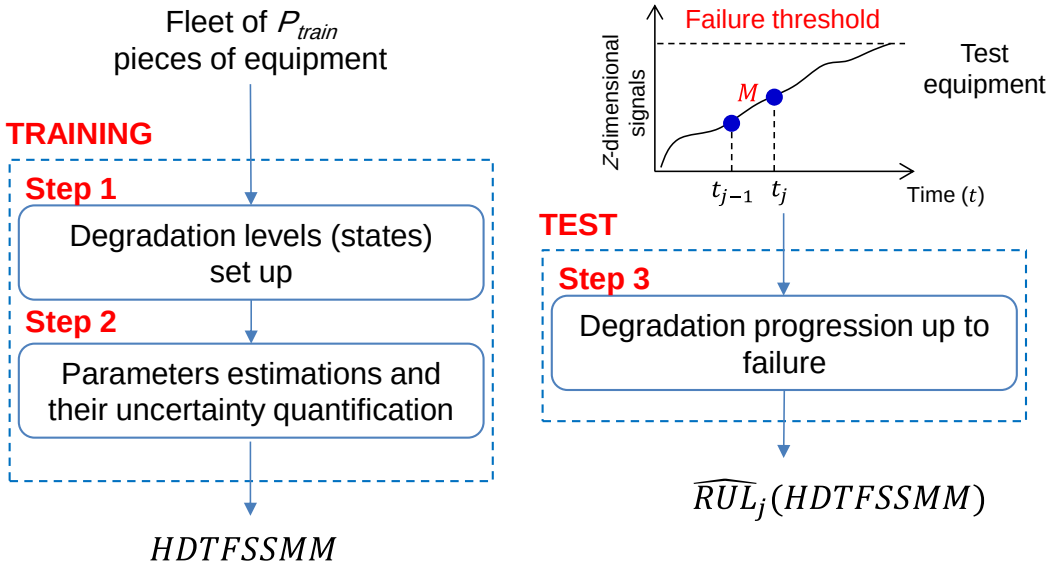

Figure 1: Flowchart of the *HDTFSSMM* model.

2.2. The Fuzzy Similarity-Based (*FSB*) model

The idea underpinning this model is to evaluate the similarity between the test trajectory and the P_{train}^c complete run-to-failure reference trajectories available, and to use the *RULs* of these latter to estimate the *RUL* of the former, considering how similar they are [24].

The flowchart for the method is sketched in Figure 2. It entails four steps:

Step 1: *Pointwise difference computation*. At the current time t_j, the distance $\delta_l^{p_{train}}$ between the sequence of the M latest measurements of the Z signals $\bar{r}_{j-M+1:j}$ of the test trajectory and all M-long segments $\bar{r}_{l-M+1:l}^{p_{train}}, l = 1, \dots, I_{p_{train}}$ of all reference trajectories $p_{train} = 1, \dots, P_{train}$ is computed:

$$\delta_l^{p_{train}} = \sum_{i=1}^{M} \left| \bar{r}_{j-M+i} - \bar{r}_{l-M+i}^{p_{train}} \right|^2 \quad (1)$$

where $|\bar{x} - \bar{y}|^2$is the square Euclidean distance between vectors $\bar{x}$ and $\bar{y}$.

Step 2: *Pointwise similarity computation*. The similarity $S_l^{p_{train}}$ of the training trajectory segment $\bar{r}_{l-M+1:l}^{p_{train}}$ to the test segment is defined as a function of the distance measure $\delta_l^{p_{train}}$. In [24], the

following bell-shaped function has turned out to give robust results in *FSB* due to its gradual smoothness [24], [41], [42]:

$$S_l^{p_{train}} = e^{-(\frac{-ln(\alpha)}{\beta^2}\delta_l^{p_{train}{}^2})} \tag{2}$$

The arbitrary parameters α and β can be set by the analyst to shape the desired interpretation of similarity into the fuzzy set: the larger the value of the ratio $\frac{-\ln(\alpha)}{\beta^2}$, the narrower the fuzzy set and the stronger the definition of similarity. The choice of the values of α and β depends on the application and are typically optimized by trial-and-error using the trajectories of the validation set [24].

Step 3: *Weight definition*. To assign the weight $v^{p_{train}}$ given to the p_{train}-th reference trajectory accounting for how similar it is to the test segment, the maximum similarity along the p_{train}-th row of the matrix of Eq. (2) is first identified:

$$S_{l^*}^{p_{train}} = \max_{l=1,\dots,I_{p_{train}}} S_l^{p_{train}} \tag{3}$$

The weight $v^{p_{train}}$ is, then, computed resorting to the arbitrarily chosen decreasing monotone function, which guarantees that the smaller the minimum distance (the larger the similarity), the larger the weight given to the p_{train}-th reference pattern, where $p_{train} = 1, \dots, P_{train}$:

$$v^{p_{train}} = S_{l^*}^{p_{train}}\, e^{(\frac{1}{\beta}(1-S_{l^*}^{p_{train}}))} \tag{4}$$

Then, the weight $v^{p_{train}}$ is normalized:

$$v^{p_{train}} = v^{p_{train}} \Big/ \sum_{p_{train}=1}^{P_{train}} v^{p_{train}} \tag{5}$$

For the prediction of the test equipment RUL, a RUL value $\widehat{rul}_{l^*}^{p_{train}}$ is assigned to each training trajectory $p_{train} = 1, \dots, P_{train}$ by considering the difference between the trajectory failure time t_F and the last time instant t_{l^*} of the trajectory segment $\bar{r}_{l^*-M+1:l^*}^{p_{train}}$, which has the maximum similarity $S_{l^*}^{p_{train}}$ with the test trajectory:

$$\widehat{rul}_{l^*}^{p_{train}} = t_F - t_{l^*} \tag{6}$$

Step 4: *RUL estimation*. The RUL prediction of the test equipment at the current time t_j, $\widehat{RUL}_j(FSB)$, is given by the similarity-weighted sum of the values $\widehat{rul}_{l^*}^{p_{train}}$:

$$\widehat{RUL}_j(FSB) = \sum_{p_{train}=1}^{P_{train}} v^{p_{train}} \widehat{rul}_{l^*}^{p_{train}} \tag{7}$$

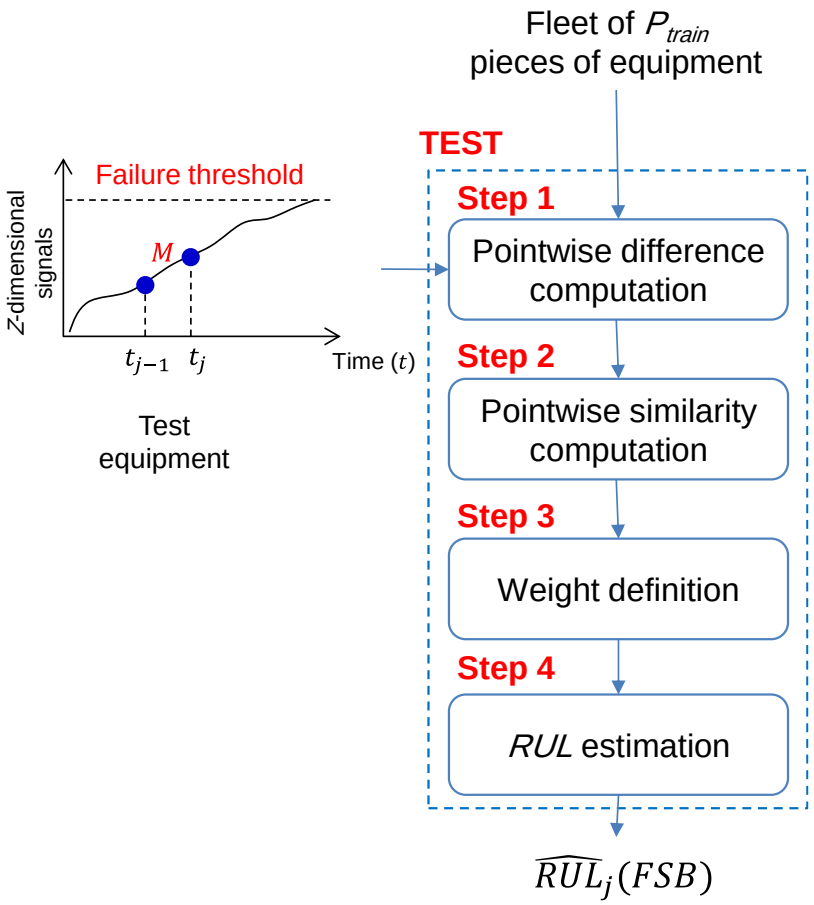

Figure 2: Flowchart of the *FSB* model.

3. The Locally Adaptive Ensemble Approach for Data-Driven Prognostics

Let us assume to have available H different prognostics models. We aggregate the *RUL* predictions for the general test trajectory by dynamically adapting the weights considering the distance of the test pattern to the patterns of a validation set P_{valid}.

More specifically, the aggregation of the prognostics models outcomes requires to associate a weight w_j^h and a bias b_j^h to the *RUL* prediction $\widehat{RUL}_j(h)$ of each model h. The basic idea consists in correcting the values of $\widehat{RUL}_j(h)$ by subtracting the estimated bias b_j^h and weighting the $\widehat{RUL}_j(h)$ with w_j^h [43]. Notice that weights and biases are different at each test time j.

The method flowchart is sketched in Figure 3. It entails five main steps:

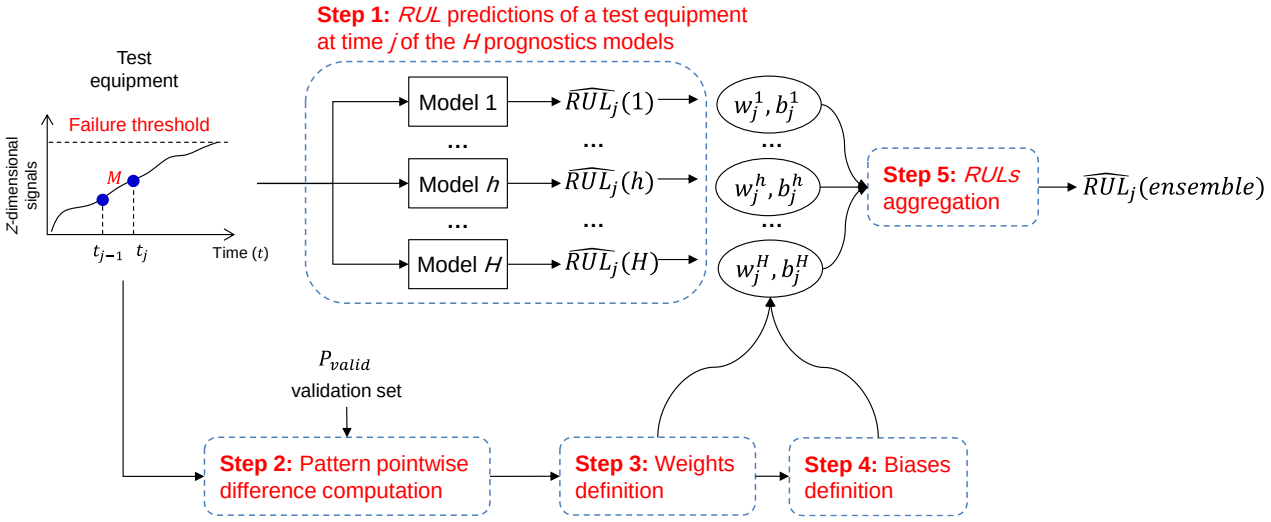

Figure 3: Flowchart of the proposed ensemble approach.

Step 1: *RUL predictions by the different prognostics models*. At the current time t_j, H *RUL* predictions $\widehat{RUL}_j(h)$, $h = 1, \dots, H$ are provided by the H prognostics models.

Step 2: *Pattern pointwise difference computation*. The distance $d_l^{p_{valid}}$ between the sequence of the M latest measurements of the Z signals $\bar{r}_{j-M+1:j}$ of the test trajectory and all M-long segment $\bar{r}_{l-M+1:l}^{p_{valid}}, l = 1, \dots, I_{p_{valid}}$ of all reference trajectories $p_{valid} = 1, \dots, P_{valid}$ is computed:

$$d_l^{p_{valid}} = \sum_{i=1}^{M} \left| \bar{r}_{j-M+i} - \bar{r}_{l-M+i}^{p_{valid}} \right|^2 \tag{8}$$

Step 3: *Weights definition.* The weight w_j^h of the h-th model is calculated based on its performance in predicting the *RUL* of the patterns of the validation set which are closer to the test pattern.

In practice, the reference pattern with the minimum distance $d_{l^*}^{p_{valid}}$ is identified for each p_{valid}-th reference trajectory as the pattern with the largest similarity to the test pattern:

$$d_{l^*}^{p_{valid}} = \min_{l=1,\dots,I_{p_{valid}}} d_l^{p_{valid}} \tag{9}$$

Since the local mean absolute error (mae) $mae_{j,P_{valid}}^h$ (defined in Eq. (10)) provides information about the performance of the h-th model in predicting the *RUL* of the P_{valid} identified patterns, it can be considered an estimation of the error that will affect the *RUL* prediction of the h-th model and thus be used for the calculations of the weight w_j^h:

$$mae_{j,P_{valid}}^{h} = \frac{\sum_{p_{valid}=1}^{P_{valid}} \left| \widehat{rul}_{l^*}^{p_{valid}}(h) - rul_{l^*}^{p_{valid}} \right|}{P_{valid}} \tag{10}$$

where $\widehat{rul}_{l^*}^{p_{valid}}(h)$ and $rul_{l^*}^{p_{valid}}$ are the *RUL* prediction provided by the h-th model for the pattern identified from the p_{valid} trajectory and its true *RUL*, respectively.

According to [43], three different weighting strategies have been considered:

a) weights proportional to the inverse of the mae:

$$w_j^h = \frac{1}{mae_{j,P_{valid}}^{h}} \tag{11}$$

b) weights proportional to the logarithm of the inverse of the normalized mae:

$$w_j^h = log\left[\frac{\underset{P_{valid,h}}{max} \left| \widehat{rul}_{l^*,j}^{p_{valid}}(h) - rul_{l^*,j}^{p_{valid}} \right|}{mae_{j,P_{valid}}^{h}} \right] \tag{12}$$

where $\underset{P_{valid,h}}{max} \left| \widehat{rul}_{l^*,j}^{p_{valid}}(h) - rul_{l^*,j}^{p_{valid}} \right|$ is the maximum value of the error over all patterns of the validation set P_{valid} and all models $h, h = 1, \dots, H$ [43].

c) weights are assigned according to the borda-count method [36]. The estimated local error is used to make a ranking of the different models and to assign them a score C_j^h, $1 < C_j^h < H$, according to their position in the ranking, i.e., 1 for the worst performing model and H for the best performing one:

$$w_j^h = C_j^h \tag{13}$$

Step 4: *Bias calculations.* The bias correction b_j^h of the h-th model is taken equal to the local mean error:

$$me_{j,P_{valid}}^{h} = \frac{\sum_{p_{valid}=1}^{P_{valid}} \left(\widehat{rul}_{l^*}^{p_{valid}}(h) - rul_{l^*}^{p_{valid}} \right)}{P_{valid}} \tag{14}$$

This quantity represents the accuracy of the *RUL* predictions obtained by each model h on the P_{valid} patterns of the validation set closer to the test pattern.

Step 5: *Aggregation of the RULs provided by the individual models.* Once the weights and the biases are calculated, each $\widehat{RUL}_j(h)$ is corrected by subtracting the estimated bias b_j^h and, then, combined with the others by means of a weighted average [43]:

$$\widehat{RUL}_j(ensemble) = \frac{\sum_{h=1}^{H} w_j^h . \left(\widehat{RUL}_j(h) - b_j^h\right)}{\sum_{h=1}^{H} w_j^h} \quad (15)$$

4. Aluminum Electrolytic Capacitors in Fully Electrical Vehicles Case Study

The potential benefit of using the proposed ensemble approach is demonstrated on a case study regarding an heterogeneous fleet of $P = 150$ aluminum electrolytic capacitors used in electric vehicles powertrains [34], [56]. The performance of the proposed approach in providing accurate *RUL* estimates is here compared with those of each individual model and of an alternative ensemble approach.

4.1. The available data

The main degradation mechanism of electrolytic capacitors is the vaporization of the electrolyte, whose degradation speed is largely influenced by the component working temperature [57].

During the capacitor life, the following Z=2 signals are measured:

1) $ESR^{measured}$ is a direct measurement of the component degradation.
2) the temperature T experienced by the capacitor, which represents the operating condition most influencing the degradation process of the capacitor.

Given the unavailability of real data describing the degradation of a fleet of capacitors, the degradation trajectories have been simulated by applying a physics-based model of the electrolyte vaporization [56], [58].

According to [56], the Normalized Equivalent Series Resistance ESR^{norm} is considered as a degradation indicator. The physics-based degradation model is represented by a first order Markov Process:

$$ESR_t^{norm} = ESR_{t-1}^{norm} e^{F(T_{t-1})} + \omega_{t-1} \quad (16)$$

where ω_{t-1} is the process noise at time $t-1$ and $F(T_{t-1})$ is a coefficient which defines the degradation rate of the capacitor depending from the capacitor working temperature at time $t-1$.

The equation linking the measurements to the ESR^{norm} is:

$$ESR_t^{measured} = ESR_t^{norm}.\left(a + be^{-\frac{(T_t^{ESR}-273.15)}{c}}\right) + \eta_t \quad (17)$$

where a, b and c are measurement parameters, T_t^{ESR} is the temperature at which the measurement has been performed at time t (usually different from the aging temperature that the capacitor experienced) and η_t is the measurement noise at time t [59].

The simulation of the evolution of the ESR^{norm} for a fleet of capacitors is performed by assuming an initial value equal to 100% and iteratively applying Eq. (16) with a time step equal to 1 hour. The failure time of the capacitor is defined as the time at which ESR^{norm} of the capacitor reaches the failure threshold of 200% [58].

The measured ESR values, $ESR^{measured}$, have been obtained by applying Eq. (17) to the numerically simulated degradation indicator values ESR^{norm} for arbitrary parameters values [56] and the possible temperature profiles have been simulated by taking into account the suggestions of design experts of the motor behavior [60], [61]: temperature variations experienced by the capacitors during life are mainly caused by i) the seasonality of the environmental external temperature and by ii) the aging (barely up to 10% of its initial temperature value). Therefore, the simulated temperature profiles follow an arbitrary sinusoidal function that justifies seasonality, by adding to this a shift sigmoidal function accounting for aging.

The heterogeneity among the $P = 150$ capacitors that belong to the fleet is guaranteed by considering arbitrary parameter values for the sinusoidal and the sigmoidal functions describing the operating conditions.

For clarification purposes, Figure 4 shows the simulated data of two capacitors (capacitor 1 and capacitor 2 – dark and light shade of color, respectively): Figure 4 (top) shows ESR^{norm}, Figure 4 (left bottom) shows $ESR^{measured}$, whereas Figure 4 (right bottom) shows the T profiles experienced by the capacitors. It is worth noticing that the higher is the temperature, the faster is the vaporization process due to the increase of the self-heating effects and, hence, the faster is, also the failure process as shown in Figure 4 (top, capacitor 2 – light shade of color) [56], [62].

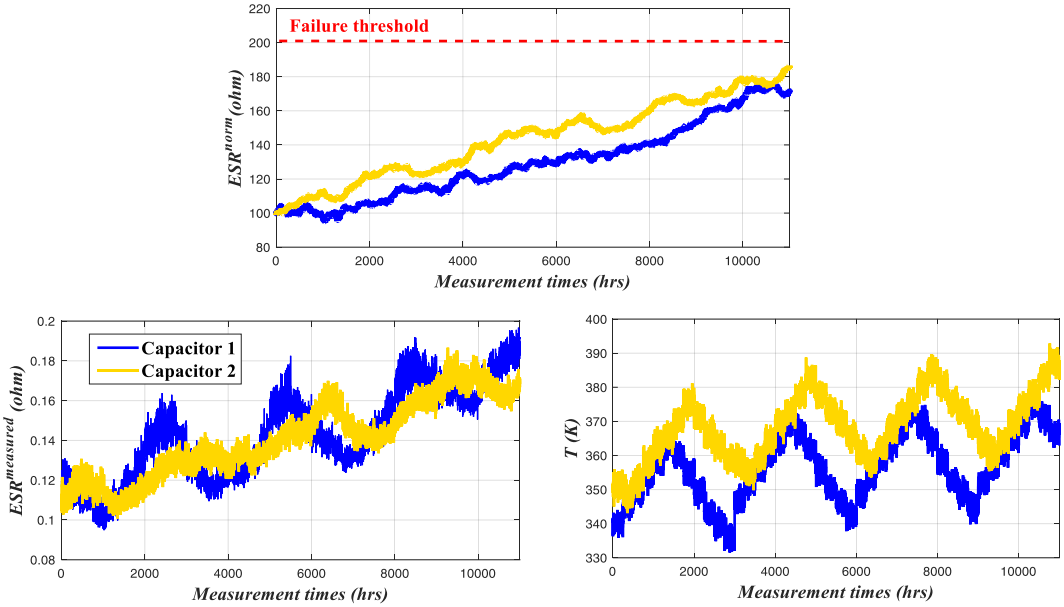

Figure 4: The true degradation process (top), the *ESR* measurements (left bottom) and the temperature profiles experienced by the capacitors (right bottom).

The whole data set is divided into $P_{train} = 100$ training, $P_{valid} = 25$ validation and $P_{test} = 25$ test trajectories. Among the $P_{train} = 100$ trajectories, $P_{train}^{c} = 20$ last all the way to the failure threshold, whereas $P_{train}^{ic} = 80$ are incomplete, i.e., measurements data are not available until failure. For clarification purposes, Figure 5 shows the ESR^{norm} of the complete and incomplete run-to-fail degradation trajectories (in dark and light shade of color, respectively).

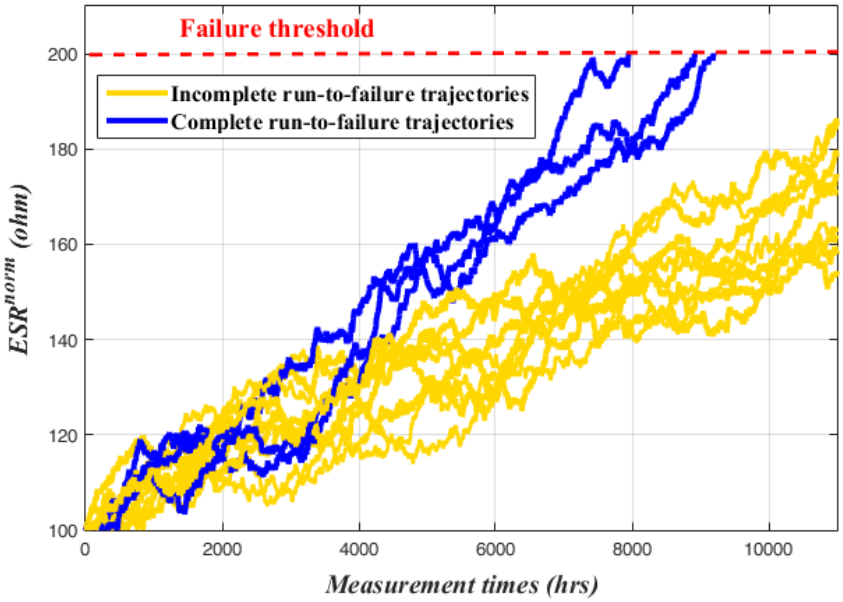

Figure 5: Examples of simulated complete and incomplete run-to-failure degradation trajectories.

All the measurements of the $P_{train} = 100$ trajectories are stored in the matrix $\bar{\bar{X}}$ that is used to build the individual models (as presented in Subsection 4.2), and thus, to develop the ensemble approach. For computational convenience, 1000 time steps between two successive measurements (i.e., $M = 1000$) are considered.

4.2. Implementation of the Ensemble Approach

The individual models are built by using the trajectories of the $P_{train} = 100$ capacitors. With respect to the *HDTFSSMM*, the whole set is used to build the degradation model and estimating its parameters, and $N_{max} = 1000$ MC trials have been used in the direct MC simulation step aimed at predicting the *RUL* of the $P_{test} = 25$ capacitors [34]. With respect to the *FSB* model, only the $P_{train}^{c} = 20$ complete run-to-failure training trajectories are used to build a reference library for estimating the *RUL* of the $P_{test} = 25$ capacitors.

Finally, for each p_{test}-th capacitor, $p_{test} = 1, \dots, P_{test}$, and at each time $t_j, j = 1, \dots, I_{p_{test}}$, the proposed ensemble approach is applied following the scheme presented in Section 3 using $P_{valid} = 25$ capacitors for the purpose of aggregating the outcomes of the individual models.

The evaluation metric considered in this work is the Accuracy Index (*AI*) [44] that is defined as the relative error of the *RUL* prediction. In practice, small *AI* values indicate more accurate predictions. The *AI* evaluation metric is defined by [44]:

$$AI^{p_{test}} = \sum_{j=1}^{I_{p_{test}}} \frac{\left|\widehat{rul}_j^{p_{test}} - rul_j^{p_{test}}\right|}{rul_j^{p_{test}}}, AI = \frac{\sum_{p_{test}=1}^{P_{test}} AI^{p_{test}}}{P_{test}} \quad (18)$$

where $AI^{p_{test}}$ and AI are the average accuracy index of the p_{test}-th equipment and of the overall P_{test} pieces of equipment, respectively.

4.3. Results

Table 1 reports the average values of the *AI* for the three alternative weight strategies and the individual models. It can be seen that the ensemble approach with any weighting scheme outperforms any of the individual model in terms of the *AI* and that the ensemble with the weight strategy b) achieves the most accurate *RUL* predictions (i.e., smallest *AI* equal to 0.37), with 42.19% improvement with respect to the best individual model, *FSB*, whose *AI* is 0.64.

	***HDTFSSMM* model**	***FSB* model**	**Locally adaptive ensemble approach**
AI	*1.24*	*0.64*	*Weight strategy a): 0.42*
			Weight strategy b): ***0.37***
			Weight strategy c): 0.47

Table 1: Value of the *AI* for the P_{test}=25 trajectories obtained by the proposed ensemble approach and the individual models.

In Figure 6 (top), the *RUL* estimates obtained by the proposed ensemble approach (weighting strategy b) for two capacitors are plotted in solid line, together with those obtained by the *HDTFSSMM* and the *FSB* in circles and squares, respectively.

The analysis of Figure 6 suggests that:

1) the predictions provided by the two models are comparable: even if the *HDTFSSMM* provides more accurate *RUL* predictions at the early stages of the capacitor life, the *FSB* model provides more accurate predictions when the capacitor approaches the end of life;

2) the ensemble of the two models, instead, allows obtaining more accurate predictions throughout the lives of the capacitors than each individual model.

Figure 6 (bottom) shows the weights dynamically assigned to the two models at each time t:

1) the *HDTFSSMM* gets a larger weight from the beginning of the lives to approximately $t = 12500$ hours compared with the *FSB* model. This can be justified by the fact that the *HDTFSSMM* exploits information taken from both the complete and the incomplete run-to-failure trajectories, whereas the *FSB* model only uses the first source of information. Furthermore, the complete run-to-failure trajectories used for training the *FSB* model are characterized by short lives (see Figure 5) and, thus, the *FSB* model tends, on average, to underestimate the capacitor *RUL* at the beginning of its degradation trajectory.
2) the *FSB* model gets exceptionally large weights towards the end of the capacitors lives compared with the *HDTFSSMM* model. This can be justified by the fact that the *HDTFSSMM* model based on a statistical model for the estimation of the Weibull distributed transition time is not effective when the capacitors approach the failure times.

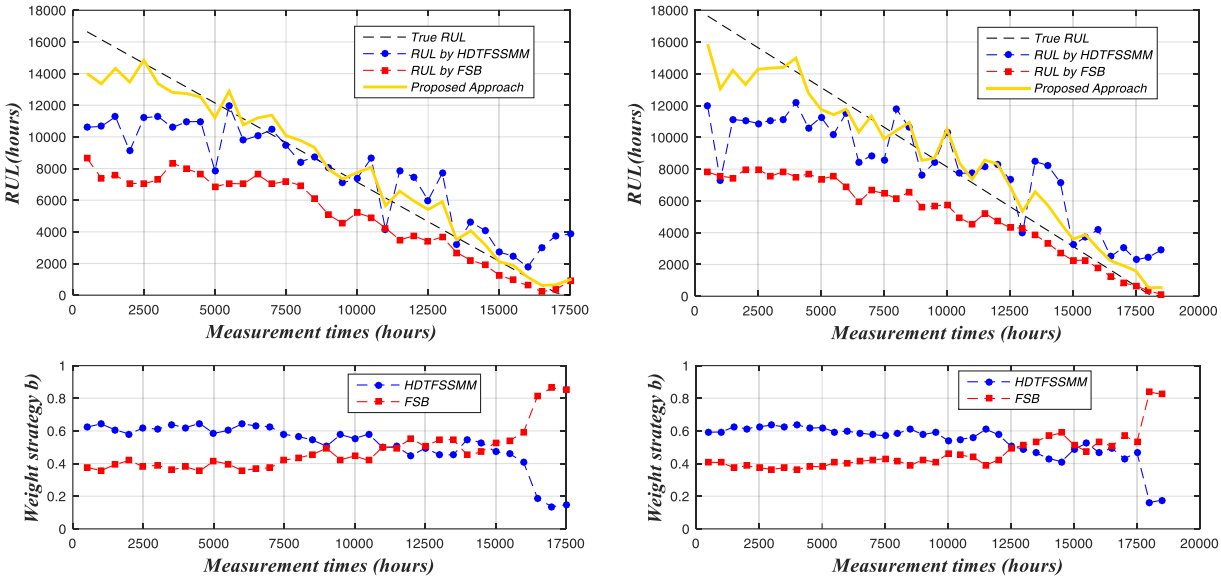

Figure 6: Comparison of the *RUL* predictions for two capacitors provided by the proposed ensemble approach and each individual model of *HDTFSSMM* and *FSB*.

On the basis of this considerations, one might argue that an alternative approach that uses only the *HDTFSSMM* for the early stage of the capacitor life and, then, only the *FSB* model might be superior (from the methodological point-of-view) and more efficient. The following Subsection 4.4 compares the performances of the proposed ensemble approach of Section 3 with that of this latter alternative, developed as in [45].

4.4. Comparison with the adaptive switching ensemble approach

The approach is structured in two phases [45]: an offline selection of the optimal switching time t_{opt} before which the *HDTFSSMM* is used for providing the *RUL* estimates and after which the *FSB* is used (the interested reader may refer to Appendix A for further details on the procedure) and an online phase that relies on t_{opt} to switch between the *HDTFSSMM* and the *FSB* for predicting the *RUL* of the $P_{test} = 25$ capacitors.

For the case of interest, by adopting a trial-and-error procedure using the validation set trajectory, t_{opt} turns out to be equal to 9000 hours.

Table 2 reports the *AI* calculated on the $P_{test} = 25$ test trajectories for the locally adaptive ensemble approach (weighting strategy b) compared with the adaptive switching ensemble approach. Notice that the proposed ensemble approach is more satisfactory, since it provides lower *AI* values.

	Locally adaptive ensemble approach (*weighting strategy b*)	**Adaptive switching ensemble approach**
AI	*0.37*	*0.51*

Table 2: Values of the *AI* for the P_{test}=25 test trajectories.

The estimates of the *RUL* obtained by the adaptive switching ensemble approach for two capacitors are shown in Figure 7 in dark solid lines before and after t_{opt} (together with those obtained by the locally adaptive ensemble approach in light solid line and each individual model in circles and squares markers). It can be easily noticed that the proposed ensemble approach outperforms the adaptive switching ensemble approach in terms of accuracy throughout the entire lives of the capacitors.

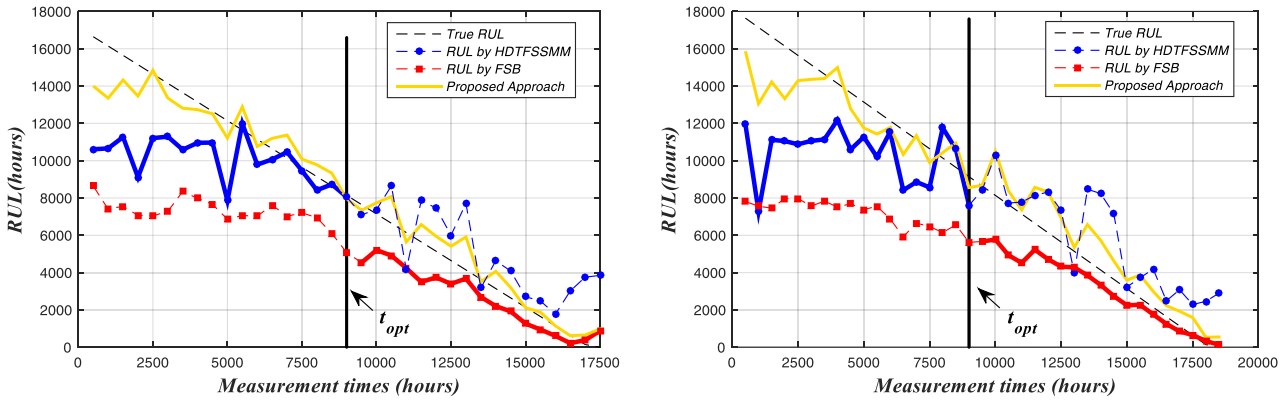

Figure 7: Comparison of the *RUL* predictions for two capacitors provided by the proposed ensemble approach, the switching ensemble approach and each single model of *HDTFSSMM* and *FSB*.

5. Conclusions

The operating conditions experienced during the life of an equipment influence both the condition monitoring data and the degradation processes. Thus, prognostics for an heterogeneous fleet of equipment working under variable operating conditions is a complex and difficult task, and prognostics approaches based on the use of individual data-driven models might not provide satisfactory predictions of the *RUL* in terms of accuracy throughout the entire life of the equipment.

In this work, we have proposed an ensemble approach based on the use of two data-driven prognostics models: an Homogeneous Discrete-Time Finite-State Semi-Markov Model (*HDTFSSMM*) and a Fuzzy Similarity-Based (*FSB*) model. The *RUL* predictions provided by the two models are aggregated using a locally weighted strategy which assigns a weight and a bias by using a measure of a local performance of the ensemble individual models, i.e., the accuracy in predicting the *RUL* of patterns of a validation set similar to the one under study.

The proposed approach is capable of i) benefiting from the availability of condition monitoring data collected from heterogeneous fleets and ii) aggregating the *RUL* predictions in an adaptive way, for good performance throughout the entire degradation trajectory of an equipment and, thus, enhancing the *RUL* estimation.

Thus, the main original contributions of this work are:

1) the application of the local fusion method developed in [43] for fault prognostics task;
2) the proposal of a new method for selecting patterns of the validation set most similar to the test pattern.

The proposed approach has been applied to a case study regarding an heterogeneous fleet of aluminum electrolytic capacitors used in electric vehicles powertrains. The performance of the proposed approach has been compared with the performance of each individual model and to an alternative ensemble approach, showing its feasibility and benefit when dealing with data collected from heterogeneous fleets.

Future work will be devoted to i) the comparison of the proposed ensemble approach to model-based prognostics approaches and to ii) the application of the proposed ensemble approach on real industrial degradation trajectories collected from the operations of a fleet of industrial equipment.

Acknowledgements

The participation of Enrico Zio to this research is partially supported by the China NSFC under grant number 71231001.

References

[1] P. Baraldi, F. Mangili, and E. Zio, "A belief function theory based approach to combining different representation of uncertainty in prognostics," *Inf. Sci. (Ny).*, vol. 303, pp. 134–149, May 2015.
[2] J. J. McCall, "Maintenance policies for stochastically failing equipment: a survey," *Manage. Sci.*, vol. 11, no. 5, pp. 493–524, 1965.
[3] Z. W., T. T., D. Z. S., and E. Z., "A dynamic particle filter-support vector regression method for reliability prediction," *Reliab. Eng. Syst. Saf.*, vol. 119, pp. 109–116, Nov. 2013.
[4] Z. Z. W. F. L. J. M. X. & W. S., "Predictive maintenance policy based on process data," *Chemom. Intell. Lab. Syst.*, vol. 103, no. 2, pp. 137–143, 2010.
[5] E. Zio, "Prognostics and Health Management of Industrial Equipment," *Diagnostics Progn. Eng. Syst. Methods Tech.*, pp. 333–356, 2012.
[6] D. Tobon-Mejia, K. Medjaher, N. Zerhouni, and G. Tripot, "Hidden Markov models for failure diagnostic and prognostic," *Progn. Heal. Manag. Conf.*, pp. 1–8, 2011.
[7] A. K. S. Jardine, D. Lin, and D. Banjevic, "A review on machinery diagnostics and prognostics implementing condition-based maintenance," *Mech. Syst. Signal Process.*, vol. 20, no. 7, pp. 1483–1510, 2006.

[8] A. Heng, S. Zhang, A. C. C. Tan, and J. Mathew, “Rotating machinery prognostics: State of the art, challenges and opportunities,” *Mech. Syst. Signal Process.*, vol. 23, no. 3, pp. 724–739, 2009.
[9] M. Bevilacqua and M. Braglia, “Analytic hierarchy process applied to maintenance strategy selection,” *Reliab. Eng. Syst. Saf.*, vol. 70, no. 1, pp. 71–83, 2000.
[10] S. Al-Dahidi, F. Di Maio, P. Baraldi, and E. Zio, “Supporting Maintenance Decision with Empirical Models Based on Fleet-Wide Data,” in *The 49th ESReDA Seminar on: Innovation through Human Factors in Risk Assessment & Maintenance, Belgium*, 2015, pp. 1–12.
[11] C. Sankavaram *et al.*, “Model-based and data-driven prognosis of automotive and electronic systems,” in *2009 IEEE International Conference on Automation Science and Engineering*, 2009, pp. 96–101.
[12] L. H. Chiang, E. Russell, and R. D. Braatz, *Fault detection and diagnosis in industrial systems*, vol. 12, no. 10–11. 2001.
[13] M. Schwabacher and K. Goebel, “A survey of artificial intelligence for prognostics,” *Assoc. Adv. Artif. Intell. AAAI Fall Symp. 2007*, pp. 107–114, 2007.
[14] X. S. Si, W. Wang, C. H. Hu, and D. H. Zhou, “Remaining useful life estimation - A review on the statistical data driven approaches,” *Eur. J. Oper. Res.*, vol. 213, no. 1, pp. 1–14, 2011.
[15] J. Z. Sikorska, M. Hodkiewicz, and L. Ma, “Prognostic modelling options for remaining useful life estimation by industry,” *Mech. Syst. Signal Process.*, vol. 25, no. 5, pp. 1803–1836, 2011.
[16] J. Lee, F. Wu, W. Zhao, M. Ghaffari, L. Liao, and D. Siegel, “Prognostics and health management design for rotary machinery systems - Reviews, methodology and applications,” *Mech. Syst. Signal Process.*, vol. 42, no. 1–2, pp. 314–334, 2014.
[17] S. Luo, J., Pattipati, K.R., Qiao, L. & Chigusa, “Model-based prognostic techniques applied to a suspension system,” *IEEE Trans. Syst. Man Cybern. Part A*, vol. 38, no. 5, pp. 1156–1168, 2008.
[18] J. Gebraeel, N., Elwany, A., & Pan, “Residual Life Predictions in the Absence of Prior Degradation Knowledge,” *IEEE Trans. Reliab.*, vol. 58, no. 1, pp. 106–117, 2009.
[19] J. Liu, W. Wang, F. Ma, Y. B. Yang, and C. S. Yang, “A data-model-fusion prognostic framework for dynamic system state forecasting,” *Eng. Appl. Artif. Intell.*, vol. 25, no. 4, pp. 814–823, 2012.
[20] E. Zio and F. Di Maio, “Fatigue crack growth estimation by relevance vector machine,” *Expert Syst. Appl.*, vol. 39, no. 12, pp. 10681–10692, Sep. 2012.
[21] J. Gebraeel, N. & Pan, “Prognostic degradation models for computing and updating residual life distributions in a time-varying environment,” *IEEE Trans. Reliab.*, vol. 57, no. 4, pp. 539– 550, 2008.
[22] Y. Li, T. R. Kurfess, and S. Y. Liang, “Stochastic prognostics for rolling element bearings,” *Mech. Syst. Signal Process.*, vol. 14, no. 5, pp. 747–762, 2000.
[23] Y. Li, S. Billington, C. Zhang, T. Kurfess, S. Danyluk, and S. Liang, “Adaptive prognostics for rolling element bearing condition,” *Mech. Syst. Signal Process.*, vol. 13, no. 1, pp. 103–113, 1999.
[24] F. Di Maio and E. Zio, “Failure Prognostics By A Data-Driven Similarity-Based Approach,” *Int. J. Reliab. Qual. Saf. Eng.*, vol. 20, no. 1, p. 1350001, 2014.
[25] V. T. Tran and B.-S. Yang, “Machine Fault Diagnosis and Prognosis : The State of The Art,” *Int. J. Fluid Mach. Syst.*, vol. 2, no. 1, pp. 61–71, 2009.
[26] W. Li and H. Pham, “An Inspection-Maintenance Model for Systems With Multiple Competing Processes,” *IEEE Trans. Reliab.*, vol. 54, no. 2, pp. 318–327, Jun. 2005.
[27] M. Schwabacher, “A survey of data-driven prognostics,” in *In Proceedings of the AIAA Infotech@ Aerospace Conference*, 2005, pp. 1–5.
[28] J. B. Coble and J. W. Hines, “Prognostic algorithm categorization with PHM challenge application,” in *2008 International Conference on Prognostics and Health Management, PHM 2008*, 2008.
[29] F. O. Heimes, “Recurrent Neural Networks for Remaining Useful Life Estimation,” *Progn. Heal. Manag. 2008. PHM 2008. Int. Conf.*, pp. 1–6, 2008.
[30] F. Di Maio, K. L. Tsui, and E. Zio, “Combining Relevance Vector Machines and exponential regression for bearing residual life estimation,” *Mech. Syst. Signal Process.*, vol. 31, pp. 405–427, Aug. 2012.
[31] G. Medina-Oliva, A. Voisin, M. Monnin, and J.-B. Leger, “Predictive diagnosis based on a fleet-wide ontology approach,” *Knowledge-Based Syst.*, vol. 68, pp. 40–57, 2014.
[32] M. Monnin, B. Abichou, A. Voisin, and C. Mozzati, “Fleet historical cases for predictive maintenance,” *The International Conference Surveillance 6, Compiègne*. .
[33] V. Agarwal, N. J. Lybeck, R. Bickford, and R. Rusaw, “Development of Asset Fault Signatures for Prognostic and Health Management in the Nuclear Industry,” *PHM, IEEE Conf.*, 2014.
[34] S. Al-Dahidi, F. Di Maio, P. Baraldi, and E. Zio, “Remaining useful life estimation in heterogeneous

fleets working under variable operating conditions," *Reliab. Eng. Syst. Saf.*, vol. 156, pp. 109–124, 2016.
[35] C. Hu, B. D. Youn, and P. Wang, "Ensemble of data-driven prognostic algorithms with weight optimization and k-fold cross validation," in *ASME 2010 International Design Engineering Technical Conferences and Computers and Information in Engineering Conference*.
[36] R. Polikar, "Ensemble based systems in decision making," *Circuits Syst. Mag. IEEE*, vol. 6, no. 3, pp. 21–45, 2006.
[37] F. Di Maio, J. Hu, P. Tse, M. Pecht, K. Tsui, and E. Zio, "Ensemble-approaches for clustering health status of oil sand pumps," in *Expert Systems with Applications*, 2012, vol. 39, no. 5, pp. 4847–4859.
[38] P. Baraldi, F. Mangili, and E. Zio, "Investigation of uncertainty treatment capability of model-based and data-driven prognostic methods using simulated data," *Reliab. Eng. Syst. Saf.*, vol. 112, pp. 94–108, Apr. 2013.
[39] F. Cadini, E. Zio, and D. Avram, "Monte Carlo-based filtering for fatigue crack growth estimation," *Probabilistic Eng. Mech.*, vol. 24, no. 3, pp. 367–373, Jul. 2009.
[40] T. Wang, J. Yu, D. Siegel, and J. Lee, "A similarity-based prognostics approach for Remaining Useful Life estimation of engineered systems," in *PHM. International Conference*, 2008, pp. 1–6.
[41] E. Zio and F. Di Maio, "A data-driven fuzzy approach for predicting the remaining useful life in dynamic failure scenarios of a nuclear system," *Reliab. Eng. Syst. Saf.*, vol. 95, no. 1, pp. 49–57, 2010.
[42] L. Angstenberger, *Fuzzy Pattern Recognition*. Kluwer Academic Publishers, 2001.
[43] P. Baraldi, A. Cammi, F. Mangili, and E. E. Zio, "Local Fusion of an Ensemble of Models for the Reconstruction of Faulty Signals," *Nucl. Sci. IEEE Trans.*, vol. 57, no. 2, pp. 793–806, Apr. 2010.
[44] A. Saxena, J. Celaya, B. Saha, S. Saha, and K. Goebel, "Metrics for Offline Evaluation of Prognostic Performance," *Int. J. Progn. Heal. Manag.*, no. 1, pp. 1–20, 2010.
[45] S. Al-Dahidi, F. Di Maio, P. Baraldi, and E. Zio, "A Switching Ensemble Approach for Remaining Useful Life Estimation of Electrolytic Capacitors," in *Proceedings of ESREL 2016*, 2016, pp. 2000–2005.
[46] M. Dong and Y. Peng, "Equipment PHM using non-stationary segmental hidden semi-Markov model," *Robot. Comput. Integr. Manuf.*, vol. 27, pp. 581–590, 2011.
[47] C. T. Chen, "Dynamic preventive maintenance strategy for an aging and deteriorating production system," *Expert Syst. Appl.*, vol. 38, no. 5, pp. 6287–6293, 2011.
[48] R. Moghaddass and M. J. Zuo, "A parameter estimation method for a condition-monitored device under multi-state deterioration," *Reliab. Eng. Syst. Saf.*, vol. 106, pp. 94–103, 2012.
[49] M. H. Shu, B. M. Hsu, and K. C. Kapur., "Dynamic performance measures for tools with multi-state wear processes and their applications for tool design and selection," *Int. J. Prod. Res.*, vol. 48, no. 16, pp. 4725–4744, 2010.
[50] R. Moghaddass and M. J. Zuo, "An integrated framework for online diagnostic and prognostic health monitoring using a multistate deterioration process," *Reliab. Eng. Syst. Saf.*, vol. 124, pp. 92–104, 2014.
[51] S. Al-Dahidi, F. Di Maio, P. Baraldi, E. Zio, and R. Seraoui, "A Novel Ensemble Clustering for Operational Transients Classification with Application to a Nuclear Power Plant Turbine," *Int. J. Progn. Heal. Manag.*, vol. 6, no. SP3, pp. 1–21, 2015.
[52] P. Baraldi, F. Di Maio, M. Rigamonti, E. Zio, and R. Seraoui, "Unsupervised clustering of vibration signals for identifying anomalous conditions in a nuclear turbine," *J. Intell. Fuzzy Syst.*, vol. 28, no. 4, pp. 1723–1731, 2013.
[53] P. Baraldi, F. Di Maio, and E. Zio, "Unsupervised Clustering for Fault Diagnosis in Nuclear Power Plant Components," *Int. J. Comput. Intell. Syst.*, vol. 6, no. 4, pp. 764–777, Aug. 2013.
[54] M. Kendall and Stuart A., *The Advanced Theory of Statistics*, vol. 2. Charles Griffin and Company limited, Lon-don & High Wycombe, 1968.
[55] M. Compare, P. Baraldi, F. Cannarile, F. Di Maio, and E. Zio, "K-Nearest Neighbour classification and homogeneous finite-state, continuous time, semi-Markov modelling for condition-based diagnostics of industrial components (under review)," *Probabilistic Eng. Mech.*, 2015.
[56] M. Rigamonti, P. Baraldi, E. Zio, D. Astigarraga, and A. Galarza, "Particle Filter-Based Prognostics for an Electrolytic Capacitor Working in Variable Operating Conditions," *IEEE Trans. Power Electron.*, vol. 31, no. 2, pp. 1567–1575, 2016.
[57] C. Kulkarni, G. Biswas, X. Koutsoukos, J. Celaya, and K. Goebel, "Integrated diagnostic/prognostic experimental setup for capacitor degradation and health monitoring," in *AUTOTESTCON*

(Proceedings), 2010, pp. 351–357.
[58] P. Venet, H. Darnand, and G. Grellet, "Detection of faults of filter capacitors in a converter. Application to predictive maintenance," *Telecommun. Energy Conf. INTELEC '93. 15th Int.*, vol. 2, pp. 229–234 vol.2, 1993.
[59] K. Abdennadher, P. Venet, G. Rojat, J.-M. Retif, and C. Rosset, "A Real-Time Predictive-Maintenance System of Aluminum Electrolytic Capacitors Used in Uninterrupted Power Supplies," *Industry Applications, IEEE Transactions on*, vol. 46, no. 4. pp. 1644–1652, 2010.
[60] A. Lahyani, P. Venet, G. Grellet, and P.-J. Viverge, "Failure prediction of electrolytic capacitors during operation of a switchmode power supply," *Power Electronics, IEEE Transactions on*, vol. 13, no. 6. pp. 1199–1207, 1998.
[61] M. L. Gasperi, "Life prediction model for aluminum electrolytic capacitors," *Ind. Appl. Conf. 1996. Thirty-First IAS Annu. Meet. IAS '96., Conf. Rec. 1996 IEEE*, vol. 3, no. 1, pp. 1347–1351 vol.3, 1996.
[62] E. Wolfgang, "Examples for failures in power electronics systems." ECPE Tutorial on Reliability of Power Electronic Systems, Nuremberg, Germany.

Appendices

Appendix A: The adaptive switching ensemble approach

The adaptive switching ensemble model [45] (sketched in Figure 8) entails, first an offline selection of the optimal switching time t_{opt} among all the possible switching times $t_{sw} = [t_{sw}^{min}, t_{sw}^{max}]$, where t_{sw}^{min} = first measurement time and t_{sw}^{max} = longest end-of-life, that minimizes the Accuracy Index (AI) over the P_{valid} validation trajectories, i.e., the relative error of the *RUL* prediction [44].

Then, an online usage for predicting the *RUL* of P_{test} pieces of equipment. In other words, the optimal switching time t_{opt} represents the time up to which *HDTFSSMM* is used for providing the *RUL* estimates at the early stage of the equipment life and beyond which *FSB* is used when the equipment approaches the end-of-life.

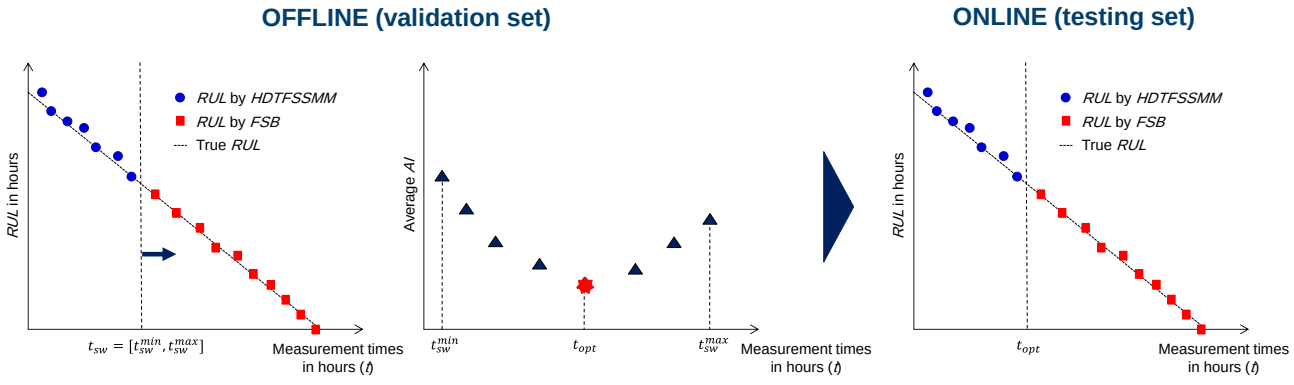

Figure 8: Flowchart of the adaptive switching ensemble approach.